J. Geophys. 48, 101–115, 1980

Journal of Geophysics

Ground-Based Observations of an Onset of Localized Field-Aligned Currents During Auroral Breakup Around Magnetic Midnight

H.J. Opgenoorth[1,2], R.J. Pellinen[1], H. Maurer[3], F. Küppers[2], W.J. Heikkila[4], K.U. Kaila[1], and P. Tanskanen[5]

[1] Finnish Meteorological Institute, Division of Geomagnetism, Vuorikatu 24, Box 503, SF-00100 Helsinki 10, Finland
[2] Institut für Geophysik der Universität Münster, Gievenbecker Weg 61, D-4400 Münster, Federal Republic of Germany
[3] Institut für Geophysik und Meteorologie der Technischen Universität Braunschweig, Mendelsohnstrasse 1 A, D-3300 Braunschweig, Federal Republic of Germany
[4] University of Texas at Dallas, Center for Space Sciences, Richardson, Texas 75080, USA
[5] Air Force Geophysics Laboratory, Hanscom Air Force Base, Massachusetts 01731, USA
(on Leave from Department of Physics, University of Oulu, Linnanmaa, SF-90570 Oulu 57, Finland)

Abstract. The substorm on 2 March 1978 was selected for study as a relatively weak substorm, starting at about local magnetic midnight, that could be observed with instruments in Northern Scandinavia. The analysis is based on a comparative study of data from the IMS magnetometer network, all-sky cameras, pulsation magnetometers, and riometers in the Scandinavian area. In addition other data are used to support the results, e.g., a photograph from the DMSP-F2 satellite, showing the auroral situation over Scandinavia, and further west, immediately after the substorm onset.

The substorm was preceded by a weak activation of aurora and magnetic disturbance about 3 min before the onset. After a fading that lasted for 20 s and could be observed only in optical aurora, the substorm onset led to a strong brightening of the aurora, an enhancement of the westward electrojet, a sudden rise in the ionospheric D-layer absorption, and Pi B type pulsations. Immediately after the onset, the ground magnetic data suggest the appearence of a pair of oppositely directed, localized, field-aligned currents (FACs). The main development of the signatures of the downward FAC was clearly delayed by about 3 min. There were significant correlations between the magnetic signatures of the two FACs and different features and spectra of the optical aurora, both in time and location. The observed Pi B type pulsations lasted as long as a growth in the local onset-connected FACs could be inferred.

Within the first three minutes the localized three dimensional current system developed into a more sheet-like configuration. An expansion to the west, possibly accompanied by a westward travelling surge, was traced with riometers and magnetometers on Iceland and Greenland.

Key words: Auroral substorm – Magnetic substorm – Substorm onset – Field-aligned currents – Auroral electrojet.

1. Introduction

The global features of magnetospheric substorms have been described in many papers (e.g. Akasofu 1964; McPherron et al. 1973; Akasofu 1974; Fukunishi 1975; Kamide and Akasofu 1975; Kisabeth and Rostoker 1974; McPherron 1979). The numerous case studies reported in these papers have led to the knowledge of substorm phenomena that we have today. However, more detailed event analyses are needed to increase our understanding of the physics involved in localized and transient effects appearing during substorms. Careful consideration of parameters such as local magnetic time, latitude, amplitude of the observed disturbance, and general magnetic activity around the event may permit a more general interpretation that can test the global picture of substorm phenomena. In this paper we shall give an example of such a study.

The coupling mechanism between the magnetospheric processes and the ionospheric phenomena observed from the ground is nowadays understood to be represented by currents driven along the magnetic field lines. Boström (1964) introduced two field-aligned current (FAC) configurations, which could possibly be responsible for the polar electrojets. In the first case (later referred to as the Boström I model), the auroral electrojet is the ionospheric closure-current between a pair of field-aligned line-currents at the eastern and western end of the electrojet, while in the second case (later referred to as the Boström II model) the auroral electrojet is the ionospheric Hall-current that is driven between a poleward and an equatorward field-aligned sheet-current. In recent literature it seems to be generally accepted that a FAC-configuration of the Boström II type exists permanently and is responsible for the quiet time eastward and westward electrojets. On the other hand, the substorm-related three-dimensional current system seems to be represented to a greater extent by the Boström I type, involving an upward FAC on the evening- and a downward FAC on the morning side of the location of substorm onset (Clauer and McPherron 1974; Iijima and Potemra 1976; Rostoker and Boström 1976; Kisabeth and Rostoker 1977; McPherron 1979).

In several magnetospheric substorm models (Atkinson 1971; McPherron et al. 1973; Akasofu 1977; Boström 1977; Heikkila and Pellinen 1977) the substorm related FAC-system is explained as being caused by deviation of the magnetospheric cross-tail current, partially closing via field lines and the ionosphere. The models differ mainly in their attempts to explain

0340-062X/80/0048/0101/$03.00

- possible trigger mechanisms for the substorm onset,
- energization of particles to the observed energies up to MeV (Pellinen and Heikkila 1978a and references therein),
- anisotropy in the precipitating particle energy spectra (Lui et al. 1977),
- well defined distribution patterns of precipitating electrons and protons (Fukunishi 1975),
- mechanisms to maintain the deviation of the cross-tail current,
- expansion of the disturbance in the neutral-sheet plane.

The ionospheric phenomena on the evening side of the expanding substorm region have already been studied to great extent. Very early scientists were attracted by such striking phenomena as the auroral westward travelling surge (WTS) (Akasofu et al. 1965a) and sharp transitions from positive to negative variation in the H-component of magnetic recordings (Heppner 1954; Harang 1946). It has been found that the area covered by the WTS can be regarded as the local area of substorm-connected electron precipitation (Akasofu et al. 1969), carrying the western upward FAC (Kamide and Akasofu 1975; Wescott et al. 1975). It forms the leading edge of the substorm-enhanced westward electrojet (Pytte et al. 1976; see also Swift 1979; McPherron 1979, and references therein).

Less is known about comparable features produced by the downward FAC on the eastern, expanding side of the substorm region. Certainly the much wider scatter of precipitating protons and positive ions (Vallance Jones 1976, p. 54) will be a reason for the lack of sharp auroral and magnetic features. Nevertheless photometer observations show a substorm related enhancement of H_β-emissions (Fukunishi 1975; Oguti et al. 1974) where the downward FAC is expected to be located (Pellinen and Heikkila 1978a).

Due to spatial limitations of instrument networks, ground-based observers have recorded the onset of a substorm mainly close to its central meridian. Since the three-dimensional current system can be expected to be quite small in extent at the very start of a substorm (Pellinen and Heikkila 1978a), it should be possible, as this study will show, to observe the features of nearly the entire onset current-system with suitably located instruments.

The studies of the local behaviour of the auroral electrojets with a meridian chain of magnetometers, in connection with other observations (Kisabeth and Rostoker 1971, 1973; Kisabeth 1972; Akasofu 1974), resulted in a better understanding of the substorm-connected current systems as well as in an improvement of analysis methods. The next step in ground-based substorm studies was the installation of a two-dimensional magnetometer array in an area that was already covered by networks of other instruments, such as all-sky cameras, riometers, photometers, pulsation magnetometers and others. This type of network was first installed by Bannister and Gough (1977, 1978) in Canada. Later Küppers et al. (1979) started a more extensive network in northern Scandinavia. The area of the Scandinavian array is sufficiently large (ca. $1{,}000 \times 1{,}000\ \mathrm{km}^2$, see Fig. 1) to cover a good portion of the entire substorm-onset phenomenon if one restricts analyses to weak or moderate substorms, recorded near to the initial onset location. As there seems to be little or no principal difference between weak and intense substorms (Kamide et al. 1975), this restriction still allows the generalization of the results.

Recently Untiedt et al. (1978) described the observation of a substorm onset near magnetic midnight with the first part of the Scandinavian IMS-network of stations. Since the auroral breakup was, in this particular case, initiated over the eastern part of their observation area, they recorded only the signatures

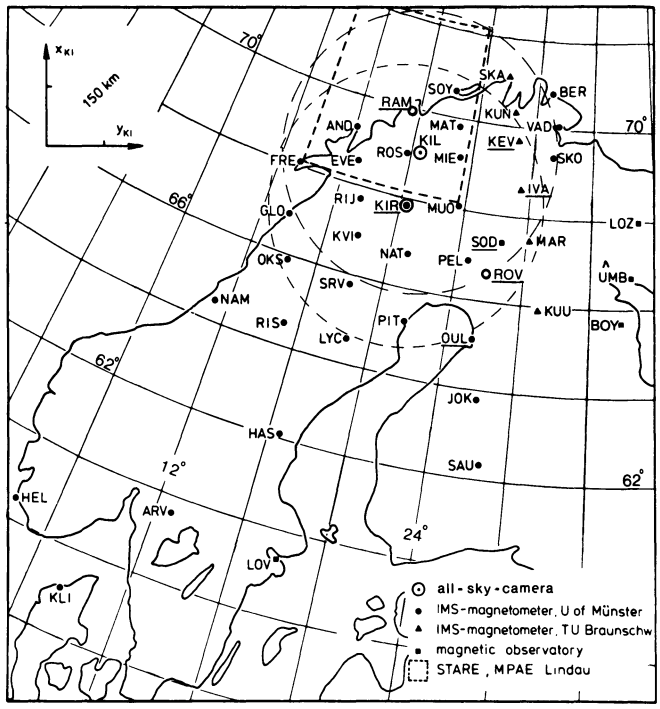

Fig. 1. Map of recording stations within the Scandinavian area from which data have been used in the present study. The different symbols that are used to indicate the various instruments are given in the right bottom corner. The stations with riometers are underlined. The observational coverage by all-sky cameras is indicated by broken circles (as defined by 15° elevation angle and 100 km height). The broken lines mark the area within which irregularity drift-velocities have been computed from the STARE-data. (for further details concerning the stations see Table 1)

of the western edge of the area of upward FAC. In the hope of recording events with the region of substorm onset being optimally located with respect to the ground-based network of stations, the so called Auroral Breakup Campaign (ABC-1) was carried out in February and March 1978 (IMS-newsletter No. 12, 1977). Of the events recorded within the three weeks of the campaign a moderate substorm that occured on 2 March 1978 was selected for the present comparative study.

In the next section we shall describe the instruments from which data has been used in our analysis. We also introduce the methods of data processing and presentation. In Sect. 3 a general overview of the geomagnetic situation during the substorm analysed will be given, followed by the description of observations during the growth phase, substorm onset, and expansion phase. In the final section we will discuss how far the observations presented are in correspondence with observations of other scientists, and whether they can be explained by the models for the magnetospheric substorm.

2. Instrumentation and Methods of Data Processing

Due to the enhanced recording activity coordinated amongst the European IMS-participants, many kinds of data-sets have been available for this study. In this section we will describe only the instruments used by the authors even though various other data have been studied and considered in the final interpretation. These

Table 1. Permanent or temporary stations from which data have been used in the present study

Station	Symbol	Geogr. coord.		Type of instrument[a] and institution[b]	
Andenes	AND	69.3° N	16.0° E	M (UM)	
Arvika	ARV	59.6	12.6	M (UM)	
Bear Island	BJN	74.5	19.2	M (AOT)	
Berlevag	BER	70.9	29.1	M (UM)	
Boyarskaya	BOY	65.8	33.8	M (PGI)	
Evenes	EVE	68.5	16.8	M (UM)	
Fredvang	FRF	68.1	13.2	M (UM)	
Glomfjord	GLO	66.9	13.6	M (UM)	
Hassela	HAS	62.1	16.5	M (UM)	
Hellvik	HEL	58.5	5.8	M (UM)	
Ivalo	IVA	68.6	27.5	M (TUB),	R (SGO)
Jokikylä	JOK	63.8	26.1	M (UM)	
Kevo	KEV	69.8	27.0	M (TUB),	R (SGO)
Kilpisjärvi	KIL	69.1	20.8		A (FMI)
Kiruna	KIR	67.8	20.4	M (UM),	A, P, R (KGI)
Klim	KLI	57.1	9.2	M (UM)	
Kunes	KUN	70.3	26.5	M (TUB)	
Kuusamo	KUU	65.9	29.0	M (TUB)	
Kvikkjokk	KVI	66.9	17.9	M (UM)	
Lavangsdalen	LAV	69.7	19.9		P (UO)
Lovö	LOV	59.4	17.8	M (SGU)	
Lovozero	LOZ	68.0	35.0	M (PGI)	
Lycksele	LYC	64.6	18.7	M (UM)	
Martti	MAR	67.5	28.3	M (TUB)	
Mattisdalen	MAT	69.9	22.9	M (UM)	
Mieron	MIE	69.1	23.3	M (UM)	
Muonio	MUO	68.3	23.6	M (UM)	
Namsos	NAM	64.5	11.1	M (UM)	
Narssarssuaq	NAR	61.2	314.6		R (DMI)
Nattavaara	NAT	66.8	21.0	M (UM)	
Okstindan	OKS	65.5	14.3	M (UM)	
Oulu	OUL	65.1	25.5	M (UM),	R (SGO)
Pello	PEL	66.9	24.7	M (UM)	
Pitea	PIT	65.3	21.6	M (UM)	
Ramfjord	RAM	69.8	19.6		R (AOT)
Risede	RIS	64.5	15.1	M (UM)	
Ritsemjokk	RIJ	67.7	17.5	M (UM)	
Rostadalen	ROS	69.0	19.7	M (UM)	
Rovaniemi	ROV	66.6	25.8		R (SGO)
Sauvamäki	SAU	62.3	26.7	M (UM)	
Skarsvag	SKA	71.1	25.8	M (TUB)	
Skogfoss	SKO	69.4	29.4	M (UM)	
Sodankylä	SOD	67.4	26.6		R (SGO)
Söröya	SOY	70.6	22.2	M (UM)	
Storavann	SRV	65.8	18.2	M (UM)	
Tjörnes	TJÖ	66.2	342.9		R (NTNF/UB)
Umba	UMB	66.7	34.5	M (PGI)	
Vadsö	VAD	70.1	29.7	M (UM)	

[a] M = magnetometer, A = all-sky camera, P = photometer, R = riometer

[b] If not explicitly explained in the text: AOT = Auroral Observatory at Tromsö, UM = University at Münster, SGU = Swedish Geological Survey, KGI = Kiruna Geophysical Institute, SGO = Geophysical Observatory at Sodankylä, TUB = Technical University at Braunschweig, PGI = Polar Geophysical Institute at Apatity, UO = University at Oslo, NTNF = Royal Norwegian Council for Scientific and Industrial Research, UB = University at Bergen, DMI = Danish Meteorological Institute, FMI = Finnish Meteorological Institute

instruments will be described later, when necessary. Results from magnetic pulsation data for this event are published elsewhere (e.g. Wedeken et al. 1979; T. Bösinger et al., paper in preparation).

The locations of the different kinds of instruments are shown in Fig. 1. More detailed information concerning the stations is listed in Table 1. During the night of 2 March 1978 two all-sky cameras (ASC) of the same design (Hyppönen et al. 1974) were operating at Kiruna and Kilpisjärvi, recording at rates of 1 frame per minute and 3 frames per minute respectively. These cameras record on 16 mm colour film, specially processed to a sensitivity of ASA 640, thus allowing an exposure time of about 2 s. The digital time display is accurate to the nearest second. Radioactive sources are used to activate calibration surfaces, visible on each photograph, for calibrations in both the red and the green part of the spectrum.

Distinct auroral structures in the ASC-pictures have been digitized along their lower borders, rectified and mapped under the assumption of a normal height of 100 km (Boyd et al. 1971).

Where possible, the final locations of aurorae have been averaged over the results of both cameras. The error in the location of the auroral forms so derived is less than 20 km, according to our experience with several stations (Opgenoorth 1978).

Data from 36 stations of the IMS-magnetometer network in Scandinavia have been used in the present study. A detailed description of this network and of the instrument types has recently been given by Küppers et al. (1979) and Maurer and Theile (1978). Additional instruments run by observatories or other institutions that were used in this study are given in Fig. 1 and Table 1.

The magnetic as well as the auroral data will be presented in a special cartesian coordinate-system, the so called KIRUNA-system. This was introduced by Küppers et al. (1979) for easier display and processing of data from the Scandinavian area. The system is centered at Kiruna in a plane tangent to the globe at the same location. The familiar horizontal components H and D are rotated to A and B respectively; B is parallel to the y_{Ki}-axis which is the tangent to the revised corrected geomagnetic latitude in Kiruna (Gustafsson 1970), A is orthogonal to B along the x_{Ki}-axis, and Z remains unchanged. The use of the KIRUNA-system in a number of studies (e.g. Untiedt et al. 1978; Baumjohann et al. 1978) showed good results in reducing the geometrical effects while the physical effects become clearer.

The magnetic disturbance vectors have been determined in comparison to a baseline which has been taken in the early morning hours of two quiet days before and after the considered night, in order to avoid Sq-effects. The data will be presented mostly in the form of so-called equivalent current vectors (TEC = *t*otal *e*quivalent *c*urrent), derived by turning the horizontal magnetic disturbance vector clockwise through 90° The vertical component will be indicated by different symbols for positive and negative variations or by isolines.

The need to differ between quiet-time current-systems and substorm-connected ones, as well as the need to recognize the character of changes in an existing current-system, made the use of so-called differential equivalent current vectors (DEC) necessary. The basic idea of this method is the assumption that a current system observed at a time t_1 stays constant until a time t_2, while an additional current system develops during the same time interval. According to the free superposition of magnetic fields, the difference between the magnetic disturbance field at the time t_2 and the field at the time t_1 can be regarded as the relatively independent effect of the new current system. The final result is naturally very much dependent on a reasonable choice of the times t_1 and t_2. However, even when the current system at the time t_1 does not stay constant until t_2 the patterns of the resulting DEC-vectors still reveal clearly the changes in the pre-existing system (e.g. Fig. 4). It should be pointed out that, due to the implied ambiguity, DEC-vectors have to be interpreted with care. In most cases other data (e.g. optical observations) allow restriction of the various possible causes of a certain pattern. The idea of splitting the total magnetic disturbance field was first introduced in the analysis of magnetic-latitude profiles by Kisabeth and Rostoker (1973) to study the small scale magnetic effects connected with auroral loops and surges. It was later applied by Untiedt et al. (1978) to data from a two-dimensional magnetometer array, and has shown its power in separating transient local phenomena from the more intense global magnetic disturbances.

Other ground based data considered in the analysis of the present event were available from the Danish Ionlab riometer network (Stauning 1978), the riometer operated in Kiruna, the Finnish chains of riometers (for technical details see Ranta 1978) and pulsation magnetometers, and the *S*candinavian-*T*win-*A*uroral-*B*ackscatter-*R*adar (STARE) at Hankasalmi, Finland and Trondheim, Norway (Greenwald et al. 1978). Unfortunately the observation area of STARE was slightly too far to the north for the special aims of this study. A meridian scanning photometer equipped with filters for measuring the wavelengths 486.1 nm (H_β), 490.7 nm (N_2^+), 630.0 nm (O_1), and 480.1 nm (background) was in operation in Kiruna, in addition to the all-sky camera. Because of the change of filters, the time resolution for this instrument was 4 min for a constant elevation. A faster, 4-channel, simultaneous-scanning photometer was operated in Lavangsdalen (Norway), but some operational changes during the time interval considered restricted the use of the data for our purposes.

Due to fortunate circumstances the ground-based data can be supported by a photograph from the DMSP-F2 satellite taken during a pass over Scandinavia (pass. no. 3837) with a camera scanning perpendicular to the satellite orbit (see Fig. 6). The picture shows the auroral situation over Scandinavia at about the time of the substorm onset, and the situations over Iceland and Greenland at later times. The movement of the sub-satellite point could be used to infer a time axis. The given coordinates have been corrected to a sphere at the altitude of the visible auroral forms, i.e. 100 km, with allowance for the varying aspect angles of the scanning camera. A more detailed description of the use of DMSP-satellite data has been given by Pike and Whalen (1974) and Eather (1979).

3. Observations

General Situation

The substorm analysed from the night of 2 March 1978, between 2200 and 2300 UT, is not isolated in the classical sense, but well separated from other activations in the course of the night. It's clear and distinct features also support the assumption that it is independent from the previous substorm, which started around 1830 UT.

This earlier substorm has a duration of more than two hours, reaching an intensity of about 500 nT. During this time considerable auroral activity is observed north of Scandinavia. Also, the main part of the substorm-connected westward electrojet is situated north of the area of observation. After these preceding substorm activities, the magnetic disturbances at stations all along the nightside of the auroral oval return to almost zero level until 2200 UT Correspondingly, auroral observations for that time show clear dark sky.

In Fig. 2 the three components of magnetograms along profile 4 (i.e., from SOY to SAU) including BJN are plotted in a stacked form to give an overview over the magnetic signatures of the substorm studied in this paper. It should be noted that they are relatively weak, reaching a maximum intensity at MUO of only 200 nT The onset of the substorm can be recognized by the sudden deflections of all components at about 2223 UT The disturbance is very localized and at that time restricted mainly to the Scandinavian area. Only later, in the course of the substorm expansion-phase, do magnetic stations further east (e.g., Dixon, USSR) and west (e.g., Leirvogur, Iceland) record the start of a negative H-bay (data not shown here). At stations in mid-latitudes and even sub-auroral latitudes, the effects of this substorm are too small to permit a reliable analysis.

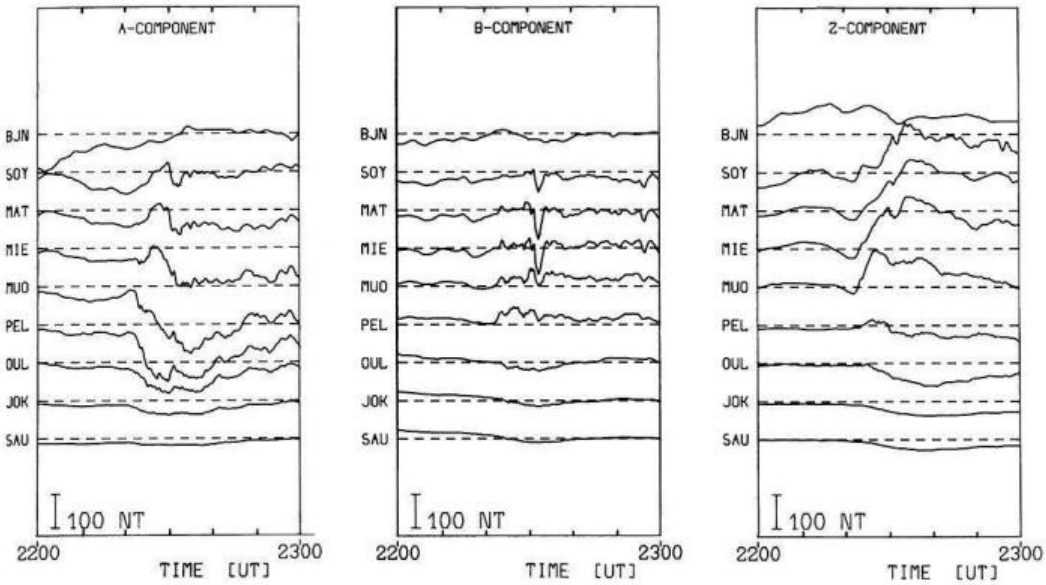

Fig. 2. Magnetic variations on 2 March 1978 from 2200 to 2300 UT at stations along a meridian. *A* and *B* denote horizontal components parallel to the x_{Ki} – and y_{Ki} – axis respectively. *Z* is positive downwards. *Horizontal lines* indicate undisturbed levels (see Sect. 2)

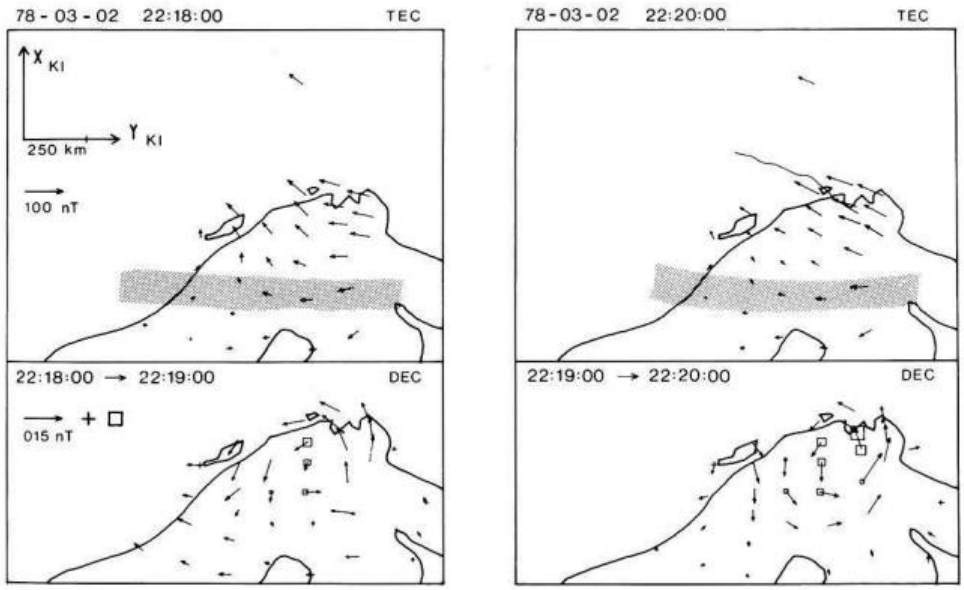

Fig. 3. Total horizontal equivalent current vectors at stations within Scandinavia before and after the appearance of a new discrete auroral form (aurora indicated by *solid lines* and *shaded area*) (*upper panels*).

Differential equivalent current vectors for the two minutes during which the new auroral form becomes appearent and grows in intensity. The vertical components are indicated by the size of the station symbol (□ = negative, + = positive) (*lower panels*)

Prephase

Before the actual substorm onset, very faint growth-phase phenomena can be observed. Soon after 2200 UT a very weak westward equivalent current starts to grow slowly in intensity. At the same time a broad, diffuse auroral band becomes visible in the ASC-pictures and the Lavangsdalen photometric recordings, extending from the western to the eastern border of the observation area. The location at 2218 UT, as shown in Fig. 3 (upper left panel), is about $x_{Ki} = -50$ to -150 km. After 2218 UT some discrete, but nevertheless still faint auroral forms suddenly appear over northern Norway. This change in auroral activity causes no clear response in the total equivalent current vectors (Fig. 3, upper right panel).

It is more interesting to look at the DEC-vectors for the time interval during which the discrete aurora appears (Fig. 3, lower panels). They show that a circular, fully closed, equivalent current with a counterclockwise sense of rotation is added to the pre-existing current system at approximately the position of the new aurora. From the ASC-pictures it cannot be clearly deduced that the development of the new auroral form takes about 2 min, as should be expected from the DEC-patterns. The Lavangsdalen

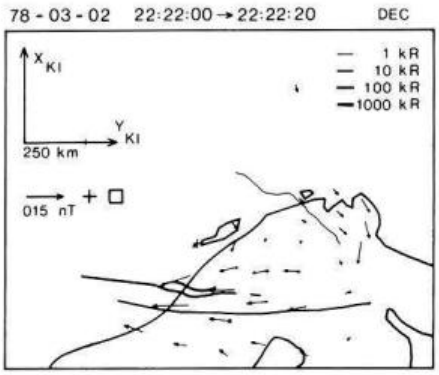

Fig. 4. Horizontal components of the differential equivalent current vectors for a 20 s interval of sudden auroral brightening. (The *brightened aurora* is represented by *solid curves* of different thicknesses, indicating different intensities.)

photometer, however, reveals that, in fact, the growth in the 557.7 nm intensity is 3 kR from 2228 to 2219 UT and still 2 kR from 2219 to 2220 UT. Referring to the papers by Fukushima (1976) and Untiedt et al. (1978) such a ground magnetic signature may be attributed to an onset of a localized upward FAC and the associated current flow in the ionosphere. Due to the ambiguity of DEC-vectors, a switch-off of a localized downward FAC could also be responsible for the same pattern. In this case the concurrent observation of the appearance of a new discrete aurora, with good correlation in time and location, makes it possible to decide that the feature observed in the DEC-vectors is most likely to be produced by a localized upward FAC, carried by precipitating electrons, which also excite the observed auroral emission.

At 2222:00 UT the diffuse band further to the south brightens and develops into discrete auroral arcs, as shown in Fig. 4; the DEC-vectors for this time interval are shown in the same figure. They reveal that, at this time, the magnetic ground signature at the position of the auroral brightening is due to a pure enhancement of the westward electrojet without a perturbation in the B-component. In the meantime the equivalent current in the northeast decreases.

Substorm Onset

Immediately before the aurora breaks up, the southernmost arc fades again for a very short time of about 20–30 s. This fading can be seen in the ASC-photograph at 2222:43 UT in Fig. 5. Perhaps due to the very short time and narrow latitudinal extent of the fading, no corresponding features in the magnetic recordings can be uniquely indentified.

The start of the breakup over Scandinavia can be fixed by ASC-data to shortly after 2222:43 UT (see Fig. 5). It starts clearly to the west of the observation area and expands very fast at first in a longitudinal direction. Even though we observe, in this case, only the eastward expansion, it seems reasonable to assume that the same effect happens on the western side as well. Since this longitudinal expansion along the brightening arc occurs within approximately 40 s it would probably appear in ASC-data with 1 min time resolution as an instantaneous brightening of the equatorward arc, as reported by Akasofu (1964). The northward expansion speed of the aurora immediately after the breakup is about 2 km/s, later decreasing to 1 km/s, according to the digitized ASC-data. The northward expansion over western Scandinavia can also

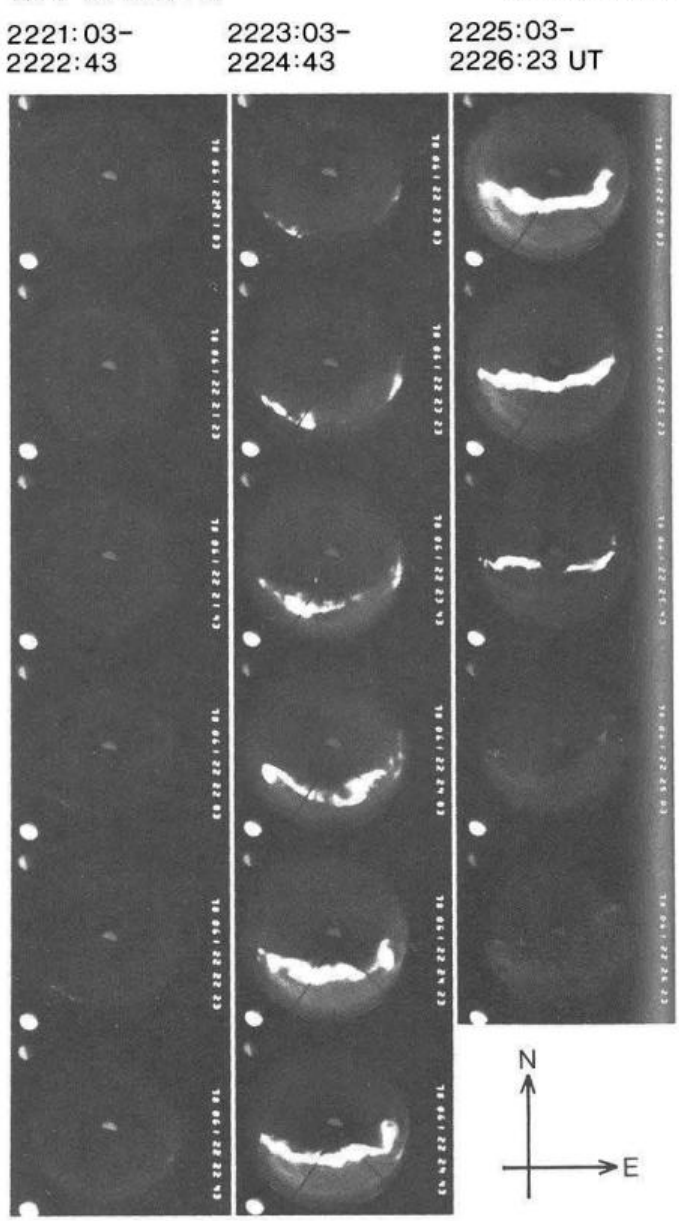

Fig. 5. All-sky camera photographs at Kilpisjärvi, Finland, for the time interval discussed on March 2, 1978

be recognized in the DMSP-picture in Fig. 6. From the picture it is possible to see that the main part of the intense aurora, and thus probably the initial location of the breakup, lies west of the Norwegian coast at about 0°–5° eastern geographical longitude, i.e., very close to local magnetic midnight (Whalen 1970).

The auroral breakup is accompanied by a strong burst of Pi-type pulsations (T. Bösinger, private communication) and a sudden increase in the ionospheric D-layer absorption. The riometer recordings in Fig. 7 show that the sharpest absorption onset occurs simultaneously with the auroral breakup and is only recorded by stations at the same latitude, i.e., Kiruna and Ivalo. A comparison of shape and amplitude of the onset at both stations supports the idea that the main area of particle precipitation lies nearer to Kiruna than Ivalo and may possibly correspond to the area of initial auroral breakup. It should be noted that the enhancement

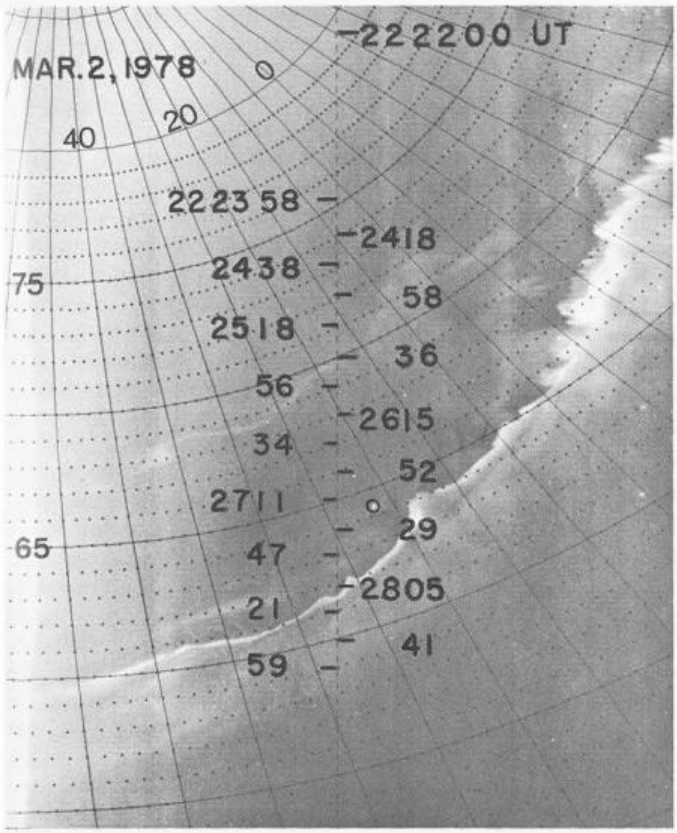

Fig. 6. Photograph from the DMSP-F2 satellite taken over the area between Scandinavia (*upper right corner*) and Greenland (*left side*) at about the time of the substorm onset. The city lights of Reykjavik are encircled, The time axis refers to the movement of the sub-satellite point. The coordinates are corrected for a height of 100 km above the earth's surface

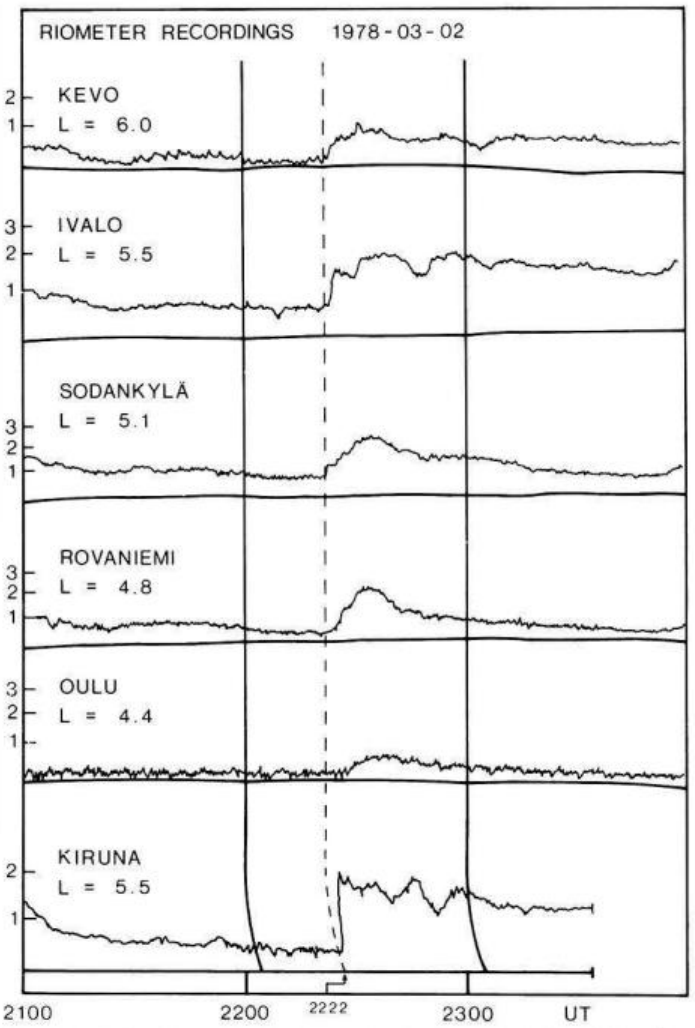

Fig. 7. Relative ionospheric absorption during the night of March 2, 1978 recorded by some riometers within the Scandinavian area. (The curve from Kiruna is taken from a different type of strip-chart recording as can be seen from the curved time marks.)

of the diffuse arc at 2222:00 UT (Fig. 4) may correspond to the smaller absorption onset observed at Sodankylä, slightly before the main absorption increase.

In Fig. 8 the total equivalent current systems before and after the substorm onset are shown. The TEC-vectors at 2222:00 UT (upper panel) are strongest in the vicinity of the visible aurora. The electrojet is still clearly separated into two major portions, but, as pointed out before, the southern portion grows towards the onset, while the northern one decreases. About two minutes after the onset at 2225:00 UT (lower panel) the westward equivalent current flow at the latitude of the auroral intensification is drastically enhanced.

To get an idea about the current system that is directly related to the breakup, and superposed on the pre-existing one, it is again reasonable to consider the DEC-system, based on the time of the moment when the aurora faded prior to the breakup, i.e., 2222:40 UT. The time by which a new current system has possibly developed seems at first glance to be 2225:20 UT, when the aurora reaches it's first maximum in northward expansion and increase of brightness. The resulting DEC-vectors in Fig. 9 (central panel) show, in the western part, a distinct U-shaped equivalent-current loop around the location of initial auroral intensification. The sense of rotation in this loop is counterclockwise with growing negative Z variations towards it's center. But in the northeastern part of the picture there is another equivalent current loop with a clockwise sense of rotation. Correspondingly, here the enclosed Z variation is positive. To understand the development of this system in space and time we analysed several series of DEC-vectors for varying time intervals as well as based on different starting times. Finally we were able to trace the following history of the substorm-connected equivalent current system during the first few minutes after the onset:

At the time of the auroral breakup a counterclockwise equivalent current loop develops around the location of the initial auroral intensification. The development of this loop lasts until the aurora reaches a first maximum of brightness at 2225:20 UT. The formation of the clockwise equivalent current loop starts simultaneously with the other one, but develops much more slowly. As can be seen in the right-hand panel of Fig. 9, a good portion of it still seems to be added during the interval from 2225:20 UT to 2226:20 UT, when the development of the counterclockwise loop has already finished. During the same time a decrease of auroral intensity is observed over the Scandinavian area (see Fig. 5). From the DMSP-photograph in Fig. 6 it can be seen that, at this time, there is no decrease in auroral activity further to the evening side of the auroral oval. Also, from the Kiruna ASC-data, there is some evidence for an intense aurora remaining south-west of

the Lofot islands in the vicinity of the counterclockwise current loop. The approximate position of the remaining bright aurora is indicated in Fig. 9 (right panel). Unfortunately the Kiruna city lights disturb the western part of the ASC-pictures and prevent a more exact location of the aurora in this part of the observation area. From Fig. 9 it can also be noted that the position of the clockwise equivalent current loop is north of the breakup aurora during the first minute after substorm onset and later within the area where the aurora ceases.

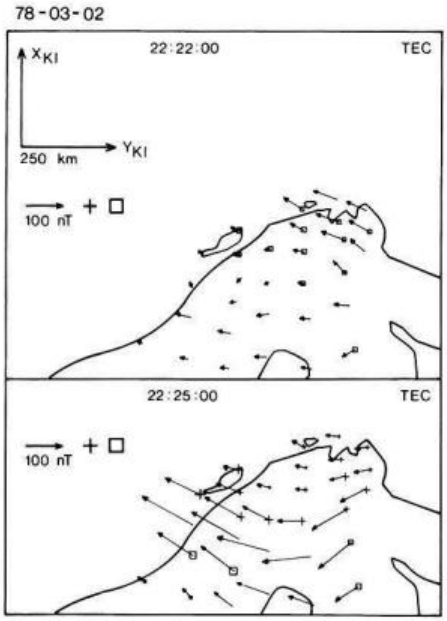

Fig. 8. Total equivalent current vectors for times before and after the substorm onset. (Vertical components again indicated by the same symbols as in Fig. 3.)

Considering the excellent temporal and spatial correlation between aurora and magnetic field as described above there must be a connection between the obviously local decrease of the intense discrete aurora and the main development of the clockwise equivalent current loop. Vice versa, there seems to exist a causal relationship between the counterclockwise equivalent current loop and the auroral breakup. But, even though a time shift in the final development of the two loops of about 2 min is obvious, it has not been possible to find a clear separation of the two loops in time. Such a separation would have indicated the possibility of a switch-on and switch-off of one and the same current system. However, in this case, the two oppositely directed equivalent-current loops clearly coexisted during the whole 3–4 min after the substorm onset. Thus it seems reasonable to consider both features as being connected with the ground signatures of the three-dimensional magnetospheric substorm onset current-system. The resulting pattern is shown by the DEC-vectors for the interval 2222:40 to 2226:20 UT in Fig. 9 (left panel).

Unfortunately the observation field of the STARE-radar does not reach far enough to the south to cover the area where the auroral breakup takes place. However, in the recordings at 2225:20 UT (shown in Fig. 10) there seems to be some evidence for a clockwise curvature in the irregularity drift-direction at the position where we observe the northern part of the counterclockwise equivalent current loop. Also, corresponding to the western part of the clockwise equivalent current loop, there is a counterclockwise irregularity drift at the same location.

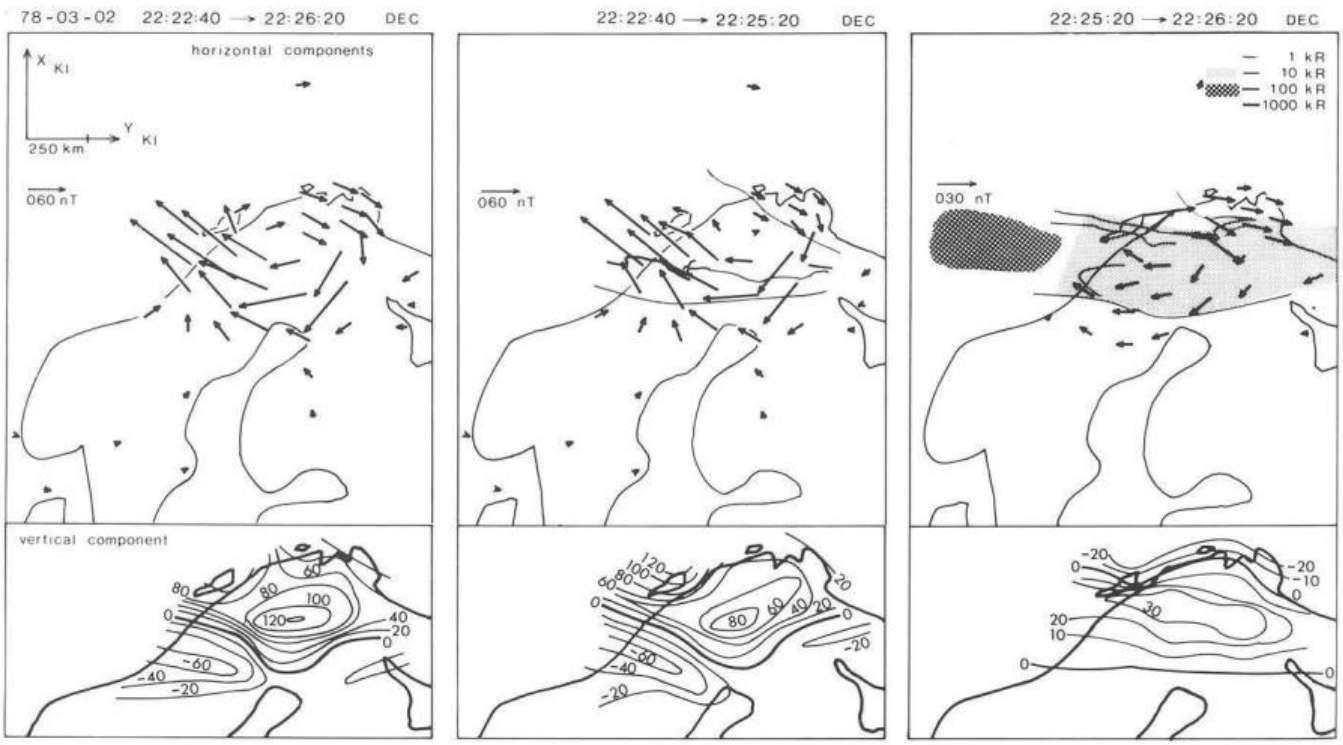

Fig. 9. Differential equivalent current vectors for selected intervals during the early time of the substorm development. The vertical components are shown separately in the lower panels by isolines computed from the values recorded at the stations. The aurorae at 2223:00 UT in the central and 2226:00 UT in the right panel are indicated by *solid curves* and *shaded areas* with intensity scaling

Expansion Phase

As pointed out in the previous chapter, the expansion speed of the aurora to the north is 2 km/s at the beginning of the breakup, and later, 1 km/s. This northward expansion of the poleward border of the visible aurora lasts until about 2235:00 UT, reaching a northernmost position of about $x_{Ki} = 400$ km. The expansion speed decreases further during the later expansion phase. Until the end of this phase the aurora enhances and decreases several times and some possibly related phenomena can be found in the magnetic data. However, most of these very local features are embedded in the simultaneous growth of the westward electrojet. A further analysis will therefore be relatively complicated and we will devote this particular study to the substorm onset.

The limited area of ASC-observation does not allow observation of substorm expansion to the east and to the west, but in the magnetic data an expansion of the equivalent current system can be traced for at least the first three minutes after the substorm onset. The clockwise loop which is (immediately after the onset) relatively small and of nearly circular shape expands to the east. A series of DEC-vectors at one minute intervals, each of them based on the end time of the previous one, (shown in Fig. 11) reveals that the equivalent current added to this loop between 2224:00 and 2225:00 UT is already oval shaped, and that the DEC-vectors for the time from 2225:00 to 2226:00 UT no longer show a closure to the east, but are, by that time, already U-shaped. During the whole development of the eastern border, both the western border of this loop and, on the opposite side, the eastern border of the counterclockwise loop stay remarkably stable. It can be concluded, therefore, that the same kind of expansion to the west takes place on the western side of the counterclockwise loop, and is not observed due to a lack of stations in that area. Baumjohann (1979) reported an expansion of the same character as shown in Fig. 11 for a counterclockwise equivalent-current loop, which had been observed in relation to a substorm onset over the eastern part of his observation area. That a westward expansion of the substorm phenomena in fact occurs in the present case as well can be deduced from the following observations further to the west.

As mentioned before, the Finnish chain of riometers, as well as the riometer at Kiruna, recorded at the time of the substorm onset a steep increase in the ionospheric D-layer absorption. The same observation was made by Stauning (1978) with his riometer at Ramfjord, Norway. However, riometers further to the west show a significant delay in the absorption onset. Figure 12 shows how the area of increased absorption expands to the west, reaching

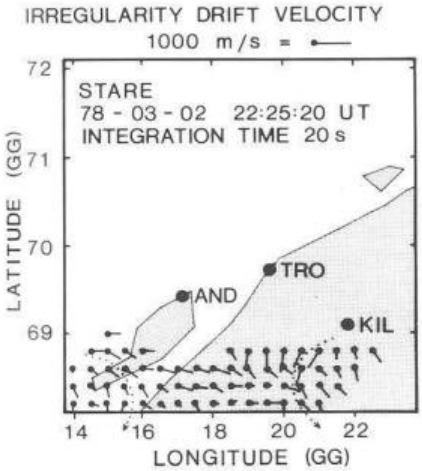

Fig. 10. Irregularity drift velocity vectors computed from the STARE-data at 2225:20 UT

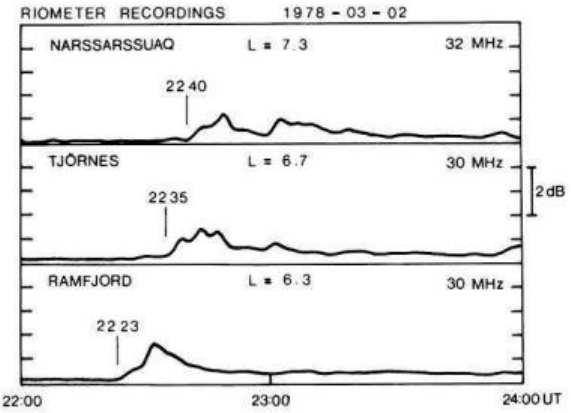

Fig. 12. Riometer recordings at stations in Scandinavia, Iceland, and Greenland on March 2, 1978 (from Stauning 1978).

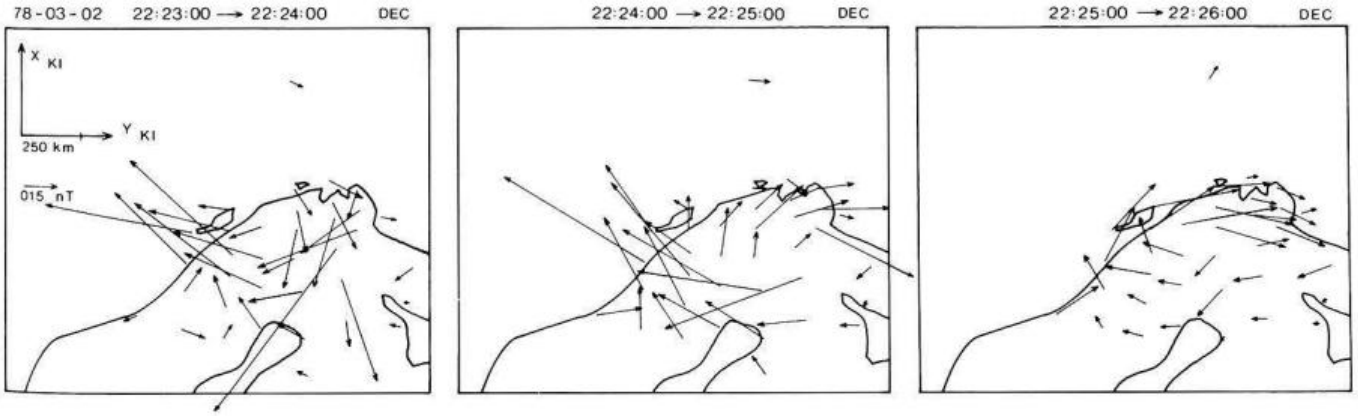

Fig. 11. Differential horizontal equivalent current vectors for three subsequent one-minute intervals during the early time after the substorm onset

Tjörnes on Iceland at about 2235:00 UT. The expansion possibly continues as far as Greenland, where the absorption over Narssarssuaq rises suddenly at 2240:00 UT. All three stations are on approximately the same geomagnetic latitude and, during this night, as can be seen from the satellite picture in Fig. 6, well situated within the auroral oval. Magnetic stations at the same location (Narssarssuaq) or very near to the riometer (Leirvogur) record the onset of a negative H bay at the same moment as the area of increased absorption arrives (data not shown here). In both cases the negative H variation is accompanied by a negative Z deviation and a sudden distortion in the D component which is clearly positive before the arrival. If one assumes that the western border of the substorm onset current system began at about 5° E geographic longitude, the resulting average expansion speed to the west would be about 1.3 km/s between Scandinavia and Iceland and about 4.5 km/s between Iceland and Greenland.

To the east, the only station from which data was available to the authors is Dixon, USSR, about 2,000 km east of Scandinavia. Here a small negative H onset was recorded at 2232:00 UT, which could possibly be related to the substorm onset over Scandinavia under discussion. Assuming the initial eastern border of the substorm onset current system at 30° E geographic longitude, this would correspond to an eastward expansion speed of about 3.4 km/s.

4. Discussion

Even though the substorm analyzed in this paper produces only very weak magnetic disturbances, it shows all the features that are known to occur during the course of a substorm of larger intensity. The clear separation from the previous intense substorm, as well as the faint growth-phase phenomena, prove that the event is independent and not an enhancement of an earlier system, as in a multiple-onset substorm reported by Pytte et al. (1976).

Development Before the Substorm Onset

The slow increase of westward equivalent current that starts after 2200:00 UT may be the result of a weak growth-phase preceding the substorm onset. Enhanced particle precipitation is indicated by the faint diffuse band of auroral luminosity that becomes visible in the ASC-pictures after about 2215:00 UT The diffuse and faint character of the visible aurora and the related westward equivalent current are not enough information to decide whether a southward movement of the aurora and the related current system takes place during the growth phase. Nevertheless the observed features clearly occur south of the latitude of the previous substorm activity.

The sudden appearance of discrete aurora at 2119:00 UT may be connected to a magnetospheric growth-phase. Several authors (Akasofu 1964; McPherron 1970; Pytte et al. 1976; Pellinen and Heikkila 1978b) have reported the observation of transient brightening or the appearance of discrete aurorae connected to small negative perturbations in the magnetic H component, taking place particularly during the growth-phase of a magnetospheric substorm. This phenomenon has been given different names, e.g., trigger bay (Rostoker 1968), pseudo-breakup (Akasofu 1964), etc., but in all cases it was believed to be of magnetospheric origin, and to be related to the same kind of instability which, in a more effective situation, leads to the onset of a real substorm. Our observations (Fig. 3) strongly suggest that these precursors are connected to a localized onset or enhancement of upward field-aligned current, which would support the opinion of the above cited authors (see also the observations of Untiedt et al. 1978).

At the second auroral intensification observed before substorm onset, taking place just after 2222:00 UT (see Fig. 4), the aurora enhances along the whole portion of the auroral oval that can be observed by our instruments, causing a pure strengthening of the westward equivalent-current flow at the narrow latitudinal region of brighter aurora. Immediately after this final auroral enhancement, before the actual onset, the auroral arc fades for a time shorter than 40 s, as can be seen from the ASC-picture at 2222:40 UT, in Fig. 5.

According to the theoretical model for substorm onset in the magnetotail by Pellinen and Heikkila (Heikkila and Pellinen 1977; Pellinen and Heikkila 1978a, b; Pellinen 1979) this fading occurs due to a localized decrease in the magnetospheric cross-tail electric field, which results in a reduction of the most effective acceleration mechanism for quiet time auroral particles, the Fermi (or curvature drift) acceleration (Sharber and Heikkila 1972). Pellinen (1979) has given a detailed description of the sequence of events that leads to auroral fading: the increase of the cross-tail current and the related thinning of the plasma sheet will be approximately linear during early times of the substorm growth phase, but, after a certain moment, the increase of the cross-tail current becomes locally non-linear. During the linear growth and the early phase of the non-linear growth, enhanced particle precipitation into the ionosphere can be observed, which results in a momentary increase in the D-layer absorption, ionospheric conductivity, and auroral brightness in a narrow latitudinal region. In fact, all these observations have been made around 2,222:00 UT

The non linearly growing cross-tail current will induce a growing electric field which is oppositely directed to the magnetospheric dawn-to-dusk field and will, after certain time, become locally stronger than the latter (Pellinen 1979). The short-lived situation of balance between the two fields will cause a momentary fading of the ionospheric phenomena associated with reduced particle precipitation (Pellinen and Heikkila 1978b). As soon as the induced electric field dominates the cross-tail electric field in a localized region of the neutral sheet, the mechanism described by Heikkila and Pellinen (1977) and Pellinen and Heikkila (1978a) may result in the onset of the actual substorm phenomena.

Field-Aligned Currents Associated With Substorm Onset

In the introduction, we have pointed out that, with a network of the type and spacing as used for this study, it should be possible to infer a good portion of the onset-connected three-dimensional current system. Based on the data presented in the previous section, we believe strongly that, in this case, our ground-based stations were situated directly under (or at least very near) the footprints of a localized pair of oppositely directed field-aligned currents, which were related to the substorm onset. Let us try to consider the magnetic and electric effects of such a pair of field-aligned currents on the ionosphere and magnetometers on the ground.

Under the assumption of homogeneous or axi-symmetric conductivity in the ionosphere, one should expect circular counter-clockwise (clockwise) ionospheric Hall-currents to be driven around the upward (downward) FAC, decreasing with growing distance from the center. In such a case only these Hall-currents

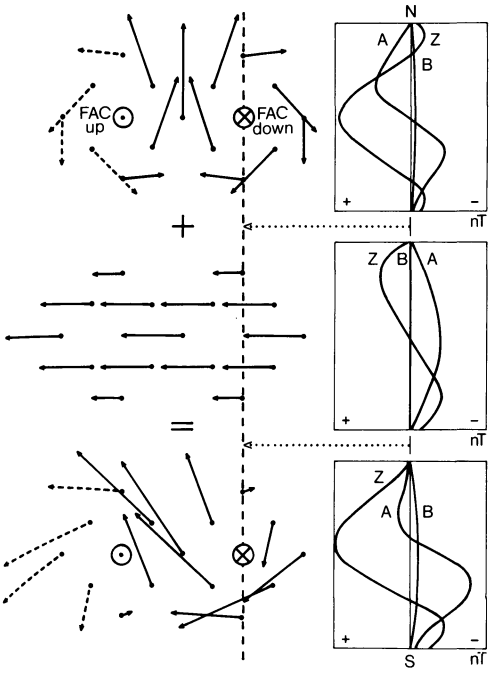

Fig. 13. Theoretical pattern of the magnetic ground effect of two vertically-incident field-aligned line-currents into a homogeneously conducting ionosphere in the forms of equivalent current vectors and a representative latitude profile (*upper panel*).

Ground perturbation of an ionospheric westward current (*central panel*). Combined ground effects of the above two panels (*lower panel*).

The chosen latitude profile is indicated by a *broken line, broken vectors* indicate the points for which no corresponding measurements could be presented in the experimentally observed pattern in Fig. 9

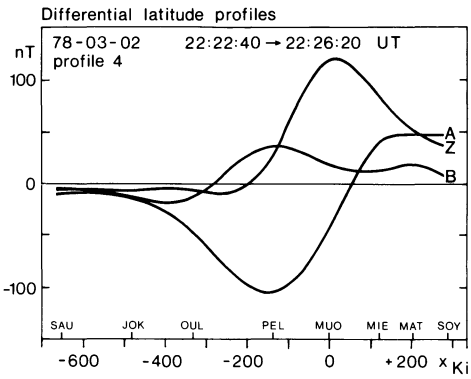

Fig. 14. Differential equivalent latitude profiles for the time interval during which the onset-connected current system develops. The meridian is located near the center of the clockwise equivalent-current loop

will produce a magnetic disturbance on the ground, while the effects of the radial Pedersen-currents, combined with the FACs, will vanish (Fukushima 1976). In Fig. 9 (left panel) two equivalent current loops can be seen, having the correct sense of rotation for the expected field-aligned current configuration at a substorm onset. The observation that, at the positions of the loops, the irregularity flow directions recorded by the STARE-radar (Fig. 10) are antiparallel to the equivalent currents supports the idea that the observed ground effect is produced by real ionospheric Hall-currents (Baumjohann et al. 1978).

Besides the two oppositely directed loops in Fig. 9, a certain asymmetry becomes apparent, which indicates the additional effect of a westward directed current. In Fig. 13 we demonstrate that, in fact, a superposition of two Hall-current loops and an additional westward current can account for the equivalent current pattern observed in connection with the substorm onset. The westward current will partly cancel the oppositely directed parts of the loop currents, while the parallel directed parts will be enhanced. The maximum and minimum of the vertical Z component will apparently be shifted to the north and south, respectively. In comparison to the theoretical latitude profiles for a meridian exactly through the center of the clockwise equivalent current loop, the observed latitude profiles for all three components along profile 4 (i.e., from SOY to SAU, see Table 1 and Fig. 1) are shown in Fig. 14. It can be seen that the observed profile is in fact very similar to the one that should be expected for the modelled superposition of a clockwise Hall-current loop and an additional westward current. The positive B-component in Fig. 14 indicates that profile 4 must be situated to the east of the clockwise loop center.

But what, in this case, is the reason for the observed westward equivalent current? The assumption of a homogeneous conducting ionosphere will not be valid for auroral latitudes, but (due to continuous particle precipitation along the auroral oval) there will always be a region of enhanced conductivity. Nevertheless, locally homogeneous conductivity will, to a first approximation, still be a reasonable assumption for the explanation of ground signatures of very localized FACs, as observed in connection with pseudo-breakups and auroral spirals, when the effective width of the FAC-connected disturbance is smaller than the latitudinal width of the auroral oval. In the case of the more intense, and possibly wider substorm onset connected FACs, however, a belt of higher conductivity has to be considered.

In a series of papers Fukushima (1974, 1975a, b) has discussed the ground magnetic effect of a single downward directed FAC which flows into a belt with Hall- and Pedersen-conductivity 3 and 2 times larger, respectively, than in the surrounding ionosphere. In order to maintain current-continuity he had to assume certain boundary conditions at the borders of the belt. The most probable conditions discussed are open field-lines at the poleward boundary, allowing secondary FAC to flow, and closed field-lines at the equatorward boundary, resulting in charge accumulation and dissipation via secondary ionospheric currents.

The basic results of his calculations are that, for such a configuration, the circular Hall-currents remain the same in principle as in the case of homogeneous conductivity, but are stronger inside the belt than outside. The Pedersen-currents, however, are no longer completely matched by the ground effect of the FAC, but have a dominating component along the belt in both directions away from the point of primary incoming FAC. If one adds to Fukushima's results the effects of an upward FAC to the west of the downward one, the resulting ground-effective Pedersen-current will be westward directed. The combined ground perturbations of the Hall- and Pedersen-currents in such a case will be somewhat similar to the pattern drafted in Fig. 13.

However, from Fukushima's numerical results it becomes clear that in all cases discussed, where the auroral-zone Hall-conductivity is larger than the Pedersen-conductivity, which according to Brekke et al. (1974) is a correct assumption, the magnetic ground perturbation caused by the ionospheric Pedersen currants will be several times smaller than the one caused by Hall-currents. Also,

other model calculations (W. Baumjohann, private communication) for a similar type of observed equivalent current pattern, assuming a conductivity channel with the ratio of Hall- to Pedersen-conductivity being 2/1, show that the westward Pedersen-current produced by a pair of field-aligned line currents alone can not account for the observed perturbation of the two Hall-current loops. Thus the only explanation for this discrepancy must be that, after the onset of the substorm, the quiet-time westward Hall-current, which is driven by the permanently existing global FAC-configuration, also increases. In fact, observations by Iijima and Potemra (1976) and Mozer (1971) have shown that the global FACs and associated electric fields do increase immediately after substorm onsets.

It should be mentioned here that all the models discussed above still neglect the inclination and curvature of the field-aligned currents, which should produce magnetic effects mainly on the equatorward side of the onset region. For a more sophisticated modelling of the real three-dimensional current configuration, the effects of currents induced in the ground have also to be considered more exactly than with only the assumption of a perfect conductor at a certain depth. In Fig. 9 (lower left panels) it can easily be seen that, e.g., the inductive coast effect is relatively strong at the Norwegian coast (station AND), producing distortions mainly in the Z component, during rapid changes in particular. Nevertheless erroneous contributions from the ground will not give rise to a wrong interpretation for the current pattern considered, the error being mostly in magnitudes.

Supporting Observations

So far we have considered only magnetic data in discussing whether the observed phenomena could have been produced by a localized pair of FACs. This is, in fact, in agreement with several other observations, as we will show below.

A sudden Pi-type pulsation burst is, according to other reports (e.g., Saito 1969; Kisabeth and Rostoker 1971, Pytte et al. 1976), very closely connected to the onset or enhancement of FAC and related ionospheric current systems. At this substorm onset a Pi-burst was observed to start simultaneously with it between 2222:00 and 2223:00 UT, to reach maximum amplitude at about 2225:00 UT, and to cease shortly after 2226:00 UT (T. Bösinger, University of Oulu, private communication). This is exactly the time interval during which we observe the development of the entire double loop system in the DEC vectors.

The very good spatial and temporal correlation between the optical auroral observations and the development of the onset-connected equivalent current system is in agreement with our interpretation. The initial auroral breakup, and later the remaining intense discrete aurora is very well situated within the counterclockwise current loop, i.e., under the upward directed FAC which should be carried mainly by energized precipitating electrons (Akasofu et al. 1969). Vice versa, the downward FAC should be carried at least to some extent by energized precipitating protons and positive ions (Potemra 1979; Klumpar et al. 1976; Pellinen and Heikkila 1978a) which are not able to produce bright aurora (Vallance Jones 1976, p. 54). This is in agreement with the observation that the aurora ceases over the Scandinavian area after 2225:20 UT, when there is still a large portion of clockwise equivalent current added to the onset-connected current system. The DMSP-photograph and the ASC-data show that this decrease in the aurora seems to be restricted to the area of probable downward FAC only.

The clear delay of about 2 min between the arrival of substorm-energized electrons (as indicated by the auroral breakup and the

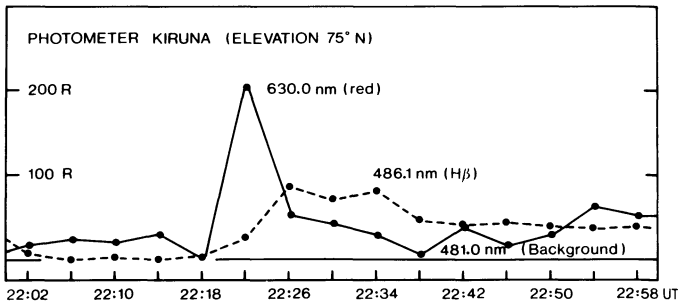

Fig. 15. Photometric recordings of the photometer in Kiruna for the wave lengths 486.1 nm (H_β) and 630.0 nm (red O_1), with background subtracted, for a representative elevation angle of 75° N. The original curve for the 630.0 nm line has been shifted 110 s back in time to correspond to the excitation of the aurora rather than its emission

counterclockwise loop representing upward FAC) and protons (as indicated by the localized cessation of the aurora and the final development and widening of the clockwise loop representing downward FAC) is an important observation. The delay had been reported earlier by Fukunishi (1975). If one accepts that the substorm onset connected energization of particles of both types must occur at the same time, by a symmetric mechanism capable of producing the observed distribution pattern, the relatively large delay in the arrival of the slower protons must mean that the energization mechanism is located far away from the earth, most probably in the magnetotail. Differences in arrival times of electron and proton beams produced in the magnetotail at substorm onset were also obtained in the simulation calculations by Pellinen and Heikkila (1978a).

Some photometric data from the instruments in Kiruna (Sweden) and Lavangsdalen (Ramfjord, Norway) show the delayed arrival of protons. The photometer at Lavangsdalen was not scanning during the time interval considered, but was viewing constantly along the magnetic field lines, i.e., towards an ionospheric region approximately over Rostadalen (ROS). The H_β-emissions from this region, which is very near to the possible location of downward FAC, start to rise after 2225:00 UT, when the visible aurora decreases in that area. Also, the photometer at Kiruna records H_β-emissions from nearly all elevation angles only some minutes after the substorm onset.

In Fig. 15 only the development of the H_β- and 630.0 nm emissions from a representative elevation angle of 75° over the northern horizon at Kiruna is shown. As we are mainly interested in comparing the moments of excitation of the two emissions, the curve for the 630.0 nm emission was shifted 110 s back in time corresponding to the average delay in the emission of this particular wavelength. Thus the two curves became approximately directly comparable, although not originally recorded synchronously. It can be seen that the rise in the H_β-emissions is preceded by a high short-lived peak of red auroral emissions, which is certainly related to the substorm onset. The entire photometric data set (not shown here) reveals that, in contrast to the H_β-emissions, this peak is observed at Kiruna only from about 40° to 90° N elevation. If one compares this observation with Fig. 9 and Fig. 14, it seems as if the red emissions are restricted to the area of initial downward FAC, while the proton-emissions observed later correspond in time and location to the final area of downward FAC, which has clearly widened and spread out further to the south. Since, according to Klumpar et al. (1976),

Kamide and Rostoker (1977), and Klumpar (1979), the downward equivalent current is carried to a large extent by upward going ionospheric electrons of low energy, the photometer observations, together with the ground signatures of localized downward FAC, give rise to some questions. It may be possible that the red auroral emissions that usually come from heights greater than 200 km (Vallance Jones 1976) have in this case been excited by upward going electrons. If this happens to be the case, it would suggest that the necessary upward directed field-aligned acceleration mechanism for ionospheric thermal electrons is related to the positive charge of the cloud of energized protons arriving from the magnetotail, as the red auroral peak is observed to decrease when the protons arrive at the ionosphere. However, the answer to this question has to be postponed until better observations are available.

The expansion of the onset-connected three-dimensional current system is in good agreement with the observations of other authors. To the west, the travelling disturbance resembles the features observed in connection with westward travelling surges (Kamide and Akasofu 1975; Kisabeth and Rostoker 1973), the speed, in the beginning at least, being of the same magnitude as given by Akasofu et al. (1965a). Figure 12 shows that the expansion of this relatively weak substorm reaches at least far as Narssarssuaq in Greenland. To the east, the expansion speed is considerably faster than to the west. The northward expansion stops after about 400 km, as reported by Akasofu et al. (1965b) for a moderate substorm.

No statement can be made on whether the central meridian of the three-dimensional substorm current system stayed stable during the whole development of expansion. According to Pytte et al. (1976) the position of the central meridian and the development of the substorm expansion can be deduced from a longitudinal profile of stations in mid-latitudes. An attempt was made to apply this method to the data from this substorm also, but due to the low intensity, the amplitudes at mid-latitudes were only of the order of nT, thus being too small to permit reliable analysis.

5. Summary and Conclusions

In this paper we reported observations of a moderate substorm with an extended network of ground-based stations. Even though the majority of the disturbances were relatively weak, the most typical features of a substorm have been observed. The results of this study can be summarized as follows:

- The extent of the IMS-network of stations in Scandinavia has proved to be close to the scale-size of substorm onset phenomena.
- The three-dimensional current system, which is connected to a substorm onset, is represented most likely by a localized pair of oppositely directed field-aligned line-currents of the configuration proposed by Boström (1964) (Boström I model).
- During the later course of the substorm, the very localized three-dimensional onset current system expands to east and west and develops into a more sheet-like configuration.
- The main magnetic ground perturbations observed at the substorm onset seem to be produced by ionospheric Hall-currents, driven by the electric fields of the local, as well as the global, field-aligned current-configurations.
- The auroral breakup is obviously related to the onset of a localized, upward directed, field-aligned current, carried by precipitating electrons, which represents the western part of the three-dimensional onset current system.
- The eastern part of the onset current system can reasonably be attributed to the effect of a downward field-aligned current. Ground based observations indicate that this downward current is carried by upward going ionospheric electrons during the first 2 min of the substorm development. Later, at least some part of this current is carried by precipitating magnetospheric protons, arriving delayed.
- For the first two minutes after the substorm onset the downward field-aligned current is well correlated with red auroral emissions, which may be excited by upward accelerated ionospheric electrons. Later the intensity of H_β-emission exceeds that of the red aurora.
- A burst of Pi-type pulsations is associated with the onset of the field-aligned currents, lasting for as long as the growth in the ground signatures of these currents can be observed.

The event reported in this paper has made us believe that we are dealing with a phenomenon characteristic of auroral substorm onset, which has never, up to now, been observed in it's entirety, even though it has been included in substorm models for a long time. We are sure that, with our experience in this study, we will be able to recognize signatures similar to our data again in the future and study them in more detail. The much better optical equipment that is planned for operation in the Scandinavian area in the future, will help us especially in clarifying some of the questions which have arisen in this study.

Acknowledgements. We wish to thank all past and present members of the magnetometer groups at the Universities of Münster and Braunschweig who were involved in collecting the magnetic data. The magnetic observations were performed in cooperation with the Aarhus University, the Department of Plasma Physics of the Royal Institute of Technology at Stockholm, the Finnish Meteorological Institute at Helsinki, the University of Bergen, the Geophysical Observatory of the Finnish Academy of Sciences and Letters at Sodankylä, the Kiruna Geophysical Institute, the University of Oulu, and the University at Tromsö. To these institutions our thanks are due for permanent support.

We also wish to thank the coordinating committee of the ABC – 1 campaign for making possible the unique data coverage, which we were able to use for the present study. We are indebted to all participants of the Second Regional IMS workshop in Bad Lauterberg, Federal Republic of Germany who took part in the first discussions concerning this particular substorm, and especially to those who supported our study with additional data, such as T. Bösinger and J. Kangas, University of Oulu, who supplied us with information about pulsations, R. Greenwald, Max Planck Institut at Lindau, who provided copies of the STARE-data, G. Gustafsson and Å. Steen, Kiruna Geophysical Institute, who sent us all-sky camera, riometer, and photometer data, K. Måseide, University at Oslo, from whom we received photometric data from Lavangsdalen, H. Ranta, Geophysical Observatory at Sodankylä, who sent us the data from the Finnish riometer chain, and P. Stauning, Danish Meteorological Institute, who made riometer data from several stations in Scandinavia, Iceland, and Greenland available to us.

The DMSP photograph was kindly provided by the Air Force Geophysical Laboratory, Hanscom Air Force Base, Massachu-

setts. The Polar Geophysical Institute at Apatity put magnetograms of stations on the Kola peninsula at our disposal.

Standard magnetograms that have been available to the authors were received from the World Data Center in Copenhagen. One of the authors (WJH) is indebted to the Atmospheric Research Section of the National Science Foundation for research support, while another (HJO) wishes to thank the Deutscher Akademischer Austauschdienst for a research grant allowing him to work in Finland.

The magnetometer array observations were supported financially by the Deutsche Forschungsgemeinschaft.

References

Akasofu, S.-I.: The development of the auroral substorm. Planet. Space Sci. **12**, 273–282, 1964

Akasofu, S.-I.: A study of auroral displays photographed from the DMSP-2 satellite and from the Alaska meridian chain of stations. Space Sci. Rev. **16**, 617–725, 1974

Akasofu, S.-I.: Physics of magnetospheric substorms. Dorndrecht, Boston: Reidel Publ. Comp. 1977

Akasofu, S.-I., Eather, R.H., Bradbury, J.N.: The absence of the Hydrogen emission H_β in the westward traveling surge. Planet. Space Sci. **17**, 1409–1412, 1969

Akasofu, S.-I., Kimball, D.S., Meng, Ch.-I.: The dynamics of the aurora II: westward traveling surges. J. Atmos. Terr. Phys. **27**, 173–187, 1965a

Akasofu, S.-I., Kimball, D.S., Meng, Ch.-I.: The dynamics of the aurora V: Poleward motions. J. Atmos. Terr. Phys. **27**, 497–503, 1965b

Atkinson, G.: Magnetosphere flows and substorms, In: Proceedings of Advanced Study Inst. on Magnetosphere Ionosphere Interactions, Dalseter, Norway 1971

Bannister, J.R., Gough, D.I.: Development of a polar magnetic substorm: A two-dimensional magnetometer array study. Geophys. J.R. Astron. Soc. **51**, 75–90, 1977

Bannister, J.R., Gough, D.I.: A study of two polar magnetic substorms with a two-dimensional magnetometer array. Geophys. J.R. Astron. Soc. **53**, 1–26, 1978

Baumjohann, W.: Spatially inhamogeneous current configurations as seen by the Scandinavian magnetometer array. In: Proceedings of the International Workshop on Selected Topics of Magnetospheric Physics. Tokyo, March 1979

Baumjohann, W., Greenwald, R.A., Küppers, F.: Joint magnetometer array and radar backscatter observations of auroral currents in northern Scandinavia. J. Geophys. **44**, 373–383, 1978

Boström, R.: A Model of the auroral electrojets. J. Geophys. Res. **69**, 4983–4999, 1964

Boström, R.: Current systems in the magnetosphere and ionosphere. In: Radar probing of the auroral plasma. A. Brekke, ed.: Proc. EISCAT Summer School, Tromsö, Norway, June 5–13 1975, Universitätsfortlaget, Tromsö-Oslo-Bergen, 1977

Boyd, J.S., Belon, A.E., Romick, G.J.: Latitude and time variations in precipitated electron energy inferred from measurements of auroral heights. J. Geophys. Res. **76**, 7694–7700, 1971

Brekke, A., Doupnik, J.R., Banks, P.M.: Incoherent scatter measurements of E region conductivities and currents in the auroral zone. J. Geophys. Res. **79**, 3773–3789, 1974

Clauer, C.R., McPherron, R.L.: Mapping the local time – universal time development of magnetospheric substorms using mid-latitude observations. J. Geophys. Res. **79**, 2811–2820, 1974

Eather, R.H.: DMSP calibration. J. Geophys. Res. **84**, 4134–4144, 1979

Fukunishi, H.: Dynamic relationship between proton and electron auroral substorms. J. Geophys. Res. **80**, 553–574, 1975

Fukushima, N.: Equivalent current pattern for a field-aligned current into the auroral belt of enhanced electric conductivity, Part I: Case of no charge accumulation at the auroral-zone boundaries. Rep. Ionos. Space Res. Jpn. **28**, 207–213, 1974

Fukushima, N.: Equivalent current pattern for a field-aligned current into the auroral belt of enhanced electric conductivity, Part II: Case of charge accumulation at the auroral-zone boundaries. Rep. Ionos. Space Res. Jpn. **29**, 31–38, 1975a

Fukushima, N.: Equivalent current pattern for a field-aligned current into the auroral belt of enhanced electric conductivity, Part III: Case of open field lines on the poleward side and closed field lines on the equatorward side of the auroral belt. Rep. Ionos. Space Res. Jpn. **29**, 39–46, 1975b

Fukushima, N.: Generalized theorem for no ground magnetic effect of vertical currents connected with Pedersen currents in the uniform-conductivity ionosphere. Rep. Ionos. Space Res. Jpn. **30**, 35–40, 1976

Greenwald, R.A., Weiss, W., Nielsen, E., Thomson, N.R.: Stare, a new radar auroral backscatter experiment in northern Scandinavia. Radio Sci. **13**, in press, 1978

Gustafsson, G.: A revised corrected geomagnetic coordinate system. Ark. Geotys. **5**, 595–617, 1970

Harang, L.: The mean field of disturbance of polar geomagnetic storms. Terr. Magn. Atmos. Electr. **51**, 353–380, 1946

Heikkila, W.J., Pellinen, R.J.: Localized induced electric field within the magnetotail. J. Geophys. Res. **82**, 1610–1614, 1977

Heppner, J.P.: Time sequences and spatial relations in auroral activity during magnetic bays at College, Alaska. J. Geophys. Res. **59**, 329–338, 1954

Hyppönen, M., Pellinen, R.J., Sucksdorff, C., Torniainen, R.: Digital all-sky camera. Technical report No. 9, Finnish Metereol. Inst. 1974

Iijima, T., Potemra, T.A.: The amplitude distribution of field-aligned currents at northern high latitudes observed by Triad. J. Geophys. Res. **81**, 2165–2174, 1976

Kamide, Y., Akasofu, S.-I.: The auroral electrojet and global auroral features. J. Geophys. Res. **80**, 3585–3602, 1975

Kamide, Y., Rostoker, G.: The spatial relationship of field-aligned currents and auroral electrojets to the distribution of nightside auroras. J. Geophys. Res. **76**, 5589–5608, 1977

Kamide, Y., Akasofu, S.-I., Deforest, S.E., Kisabeth, J.L.: Weak and intense substorms. Planet. Space Sci. **23**, 579–587, 1975

Kisabeth, J.L.: The dynamical development of the polar electrojets. Edmonton: PhD Thesis, University of Alberta 1972

Kisabeth, J.L., Rostoker, G.: Development of the polar electrojet during polar magnetic substorms. J. Geophys. Res. **76**, 6815–6828, 1971

Kisabeth, J.L., Rostoker, G.: Current flow in auroral loops and surges inferred from ground-based magnetic observations. J. Geophys. Res. **78**, 5573–5584, 1973

Kisabeth, J.L., Rostoker, G.: The expansive phase of magnetospheric substorms. I. Development of the auroral electrojets and auroral arc configuration during a substorm. J. Geophys. Res. **79**, 972–984, 1974

Kisabeth, J.L., Rostoker, G.: Modelling of the three-dimensional current systems associated with magnetospheric substorms. Geophys. J.R. Astrom. Soc. **49**, 655–683, 1977

Klumpar, D.M.: Relationship between auroral particle distributions and magnetic field perturbations associated with field-aligned currents (accepted for publication). J. Geophys. Res. 1979

Klumpar, D.M., Burrows, J.R., Wilson, M.D.: Simultaneous observations of field-aligned currents and particle fluxes in the post-midnight sector. Geophys. Res. Lett. **3**, 395–398, 1976

Küppers, F., Untiedt, J., Baumjohann, W., Lange, K., Jones, A.G.: A two-dimensional magnetometer array for ground-based observations of auroral zone electric currents during the International Magnetospheric Study (IMS). J. Geophys. **46**, 429–450, 1979

Lui, A.T.Y., Venkatesan, D., Anger, C.D., Akasofu, S.-I., Heikkila, W.J., Winningham, J.D., Burrows, J.R.: Simultaneous Observations of particle precipitations and auroral emissions by the ISIS 2 satellite in the 19–24 MLT sector. J. Geophys. Res. **82**, 2210–2226, 1977

Maurer, H., Theile, B.: Parameters of the auroral electrojet from magnetic variations along a meridian. J. Geophys. **44**, 415–426, 1978

McPherron, R.L.: Growth phase of magnetospheric substorms. J. Geophys. Res. **75**, 5592–5599, 1970

McPherron, R.L.: Magnetospheric substorms. Rev. Geophys. Space Phys. **17**, 657–681, 1979

McPherron, R.L., Russel, C.T., Aubry, M.P.: Satellite studies of magnetospheric substorms on August 15, 1968. 9. Phenomenological model for substorms. J. Geophys. Res. **79**, 3131–3149, 1973

Mozer, F.S.: Origin and effects of electric fields during isolated magnetospheric substorms. J. Geophys. Res. **76**, 7595–7608, 1971

Oguti, T., Fukunishi, H., Tohmatsu, T., Nagata, T : H_β-emissions during auroral breakup. Memoirs of National Inst. of Polar Research, Special Issue No. 3, Proceedings of antarctic review meeting, 10–20, 1974

Opgenoorth, H.J.: Vergleich von Strukturen im Polarlicht und im Magnetfeld gleichzeitiger Ionosphärenströme. Diplomarbeit Physik, Inst. f. Geophys. Univ. Münster, FRG, 1978

Pellinen, R.J.: Induction model and observations of onset of magnetospheric substorms. PhD Thesis, University of Helsinki, Finland 1979

Pellinen, R.J., Heikkila, W.J.· Energization of charged particles to high energies by an induced substorm electric field within the magnetotail. J. Geophys. Res. **83**, 1544–1550, 1978a

Pellinen, R.J., Heikkila, W.J.: Observations of auroral fading before breakup. J. Geophys. Res. **83**, 4207–4217, 1978b

Pike, C.P., Whalen, J.A.: Satellite observations of auroral substorms. J. Geophys. Res. **79**, 985–1000, 1974

Potemra, T.: Current systems in the earth's magnetosphere. Rev. Geophys. Space Phys. **17**, 640–656, 1979

Pytte, T., McPherron, R.L., Kokubun, S.: The ground signatures of the expansion phase during multiple onset substorms. Planet. Space Sci. **24**, 1115–1132, 1976

Ranta, H.: The onset of an auroral absorption substorm. J. Geophys. Res. **83**, 3893–3899, 1978

Rostoker, G.: Macrostructure of geomagnetic bays. J. Geophys. Res. **73**, 4217–4229, 1968

Rostoker, G., Boström, R.: A mechanism for driving the gross Birkeland current configuration in the auroral oval. J. Geophys. Res. **81**, 235–244, 1976

Saito, T.: Geomagnetic pulsations. Space Sci. Rev. **10**, 319–412, 1969

Sharber, R.J., Heikkila, W.J.: Fermi acceleration of auroral particles, J. Geophys. Res. **77**, 3397–3410, 1972

Stauning, P.: Compilation of Ionlab riometer data for IMS-workshop in Bad Lauterberg, FRG in October 1978. Ionlab report R51, Danish Metereol. Institute, Techn. Univ., Lungby, Denmark, 1978

Swift, D.W.: Auroral mechanisms and morphology. Rev. Geophys. Space Phys. **17**, 681–696, 1979

Untiedt, J., Pellinen, R.J., Küppers, F., Opgenoorth, H.J., Pelster, W.D., Baumjohann, W., Ranta, H., Kangas, J., Czechowsky, P., Heikkila, W.J.: Observations of the initial development of an auroral and magnetic substorm at magnetic midnight. J. Geophys. **45**, 41–65, 1978

Vallance Jones, A.: Aurora. Dordrecht, Boston: D. Reidel Publ. Comp. 1976

Wedeken, U., Hillebrand, O., Krenzien, E., Ranta, A., Ranta H., Voelker, H.: Cosmic noise absorption events and geomagnetic pulsations activity during substorms. J. Geophys. **46**, 249–259, 1979

Wescott, E.M., Stenbaek-Nielsen, H.C., Davis, T.N., Murcray, W.B., Peek, H.M., Bottoms, P.J.: The L=6.6 Oosik Barium plasma injection experiment and magnetic storm on March 7, 1972. J. Geophys. Res. **80**, 951–966, 1975

Whalen, J.A.: Auroral oval plotter and nomograph for determining corrected geomagnetic local time, latitude, and longitude for high latitudes in the northern hemisphere. Environmental Res. Papers No. 327, Air Force Cambridge Res. Lab., Bedford, Mass., 1970

Received December 12, 1979; Revised Version March 17, 1980; Accepted March 17, 1980